Research Article

Ehsan Kianpour* and Nor Azwadi Che Sidik

A Detailed Study of Row-Trenched Holes at the Combustor Exit on Film-Cooling Effectiveness

https://doi.org/10.2478/mme-2019-0033
Received Mar 26, 2018; revised Sep 10, 2018; accepted Nov 20, 2018

Abstract: To analyse the effects of cylindrical- and row-trenched cooling holes with an alignment angle of 90 degrees on the film-cooling effectiveness near the combustor end wall surface at a blowing ratio of 3.18, the current research was done. This research included a 3D representation of a Pratt and Whitney gas turbine engine, which was simulated and analysed with a commercial finite volume package FLUENT 6.2.26. The analysis was done with Reynolds-averaged Navier–Stokes turbulence model on internal cooling passages. This combustor simulator was combined with the interaction of two rows of dilution jets, which were staggered in the streamwise direction and aligned in the spanwise direction. In comparison with the baseline case of cooling holes, using row-trenched hole near the end wall surface increased the film-cooling effectiveness 44% in average.

Keywords: Gas turbine engine, Film cooling, Combustor simulator, Trench hole, Dilution hole

1 Introduction

Advanced gas turbine industries are trying for higher engine efficiencies. Brayton cycle is a key to achieve this purpose. In this cycle, to have higher gas turbine engine efficiency, the combustor's outlet temperature must increase [1]. But such hot flows cause non-uniformities at the end of the combustor and the inlet of turbine and damage the critical parts. Film cooling is the most well-known method of preservation. In this technique, a low-temperature thin layer attaches on a surface and protects it against hot streams. To get better film-cooling performance, the blowing ratio needs to be increased. Blowing ratio increment has an intense effect on the heat transfer, particularly in the hole region. Because of the importance of this study, a broad literature survey was done to get the fundamental data.

Abdullah and Funazaki [2] analysed the effects of hole angle geometries on film cooling. They considered four different rows of inclined holes with angles of 20 degrees and 35 degrees. They made ready the contours which showed the laterally averaged film-cooling distribution and cooling performance at x/D equal to 3, 13, 23 and 33. The results demonstrate that at a higher blowing ratio (BR=3.0 and 4.0), the interaction between the neighbouring secondary airs leads to a full coverage film-cooling effectiveness downstream of the fourth row, which is confirmed by the temperature field captured at x/D=33 and BR=4.0. The results also show that a higher cooling effectiveness is achieved at a shallow hole angle of ϕ = 20 degrees, especially at higher blowing ratios in comparison with a baseline with a hole angle of ϕ = 35 degrees. In line with this study, Sarkar and Bose [3] showed that the application of cooling holes with elevated injection angles enlarged the turbulence, and higher turbulence led to cooling performance degradation. In addition, Nasir *et al.* [4], Shine *et al.* [5] and Hale *et al.* [6] simulated a flat plate with cylindrical cooling holes to study the effects of injection angle on the effectiveness of film cooling. They highlighted that lower streamwise injection angles perform better to have a higher film-cooling effectiveness.

Vakil and Thole [7] presented experimental results of the study of temperature distribution inside a combustor simulator. In this study, a real large scale of combustor was modelled. This model contained four different cooling panels with many cooling holes. Two rows of dilution jets could be seen in the second and third cooling panels. The first row had three dilution jets and the second one had two jets. Whereas the first and second panels were flat, two other panels were angled with an angle of 15.8 degrees. In this study, a real large scale of combustor was simulated and high-momentum dilution jets and coolant flow were injected into the main flow. The results indicated that a high temperature gradient was developed upstream of the

***Corresponding Author: Ehsan Kianpour:** Department of Mechanical Engineering, Najafabad Branch, Islamic Azad University, Najafabad, Iran; Email: ekianpour@pmc.iaun.ac.ir
Nor Azwadi Che Sidik: Department of Thermo-fluid, Faculty of Mechanical Engineering, University Technology of Malaysia, Skudai, Johor, Malaysia

dilution holes. Kianpour *et al.* [8, 9] re-simulated the Vakil and Thole's combustor. They offered various geometries of cooling holes. The temperatures near the wall and among the jets were higher for baseline cooling, whereas the central part of the jets was cooler in trenched cases.

Using a turbine vane cascade, the effects of shallow trenched holes ($d = 0.5D$) were investigated by Somawardhana and Bogard [10] to improve the performance of film cooling. They measured the effectiveness of film cooling under blowing ratios from BR=0.4 to 1.6. The findings indicated that upstream obstructions reduced the effectiveness by 50%. However, downstream obstructions increased the film-cooling performance. The film-cooling performance was slightly affected by a combination of obstructions near the upstream obstructions. Using a narrow trench, they dramatically modified the cooling performance and reduced the effects of surface roughness decrease. The results agreed with the findings of Harrison *et al.* [11] and Shupping [12]. Furthermore, Somawardhana and Bogard showed higher film-cooling effectiveness for the trenched holes which resulted from the net heat flux reduction being higher than the baseline case, whereas the heat transfer coefficient was approximately constant for both cases. In contrast, Yiping and Ekkad [13] showed that trenching cooling holes increased heat transfer coefficient. Ai *et al.* [14] showed the results the ratio of coolant momentum and the cooling effectiveness was reduced whereas at low blowing ratios the performance became better by traditional cooling holes.

By using control volume technique and RNG k-ϵ turbulence model, Zhang *et al.* [15] investigated the flow and heat transfer behaviour on flat plate film cooling from cone-shaped and round-shaped cooling holes. They used RNG k-ϵ turbulent model to simulate the model and solve the Reynolds-averaged Navier–Stokes equation. The results showed that at the same blowing ratio, the film-cooling effectiveness is better for the cone-shaped holes than for round-shaped holes. Also, for cone-shaped jets, the jet to crossflow blowing ratio reaches an optimum condition of 1.0 to yield the best film-cooling effectiveness [16, 17]. In addition, Saumweber *et al.* [18], Saumweber and Schulz [19] and Barigozzi *et al.* [20] indicated that better thermal protection is attained at higher blowing ratios.

In agreement with the study background, several authors motivated the author to do this research. End wall of the combustor can be damaged by hot gases which flow inside a combustor simulator, and increasing the film-cooling effectiveness above these surfaces is an important issue which has attracted less attention till now. In addition, most of the studies paid attention to the using of trenched holes at the leading edge of the turbine blades and, in most of them, the application of these holes at the end wall combustor is not considered. The alignment angle of the trenched cooling holes is a topic which was not considered in the past researches. Also, this approach of cooling holes can be utilized by engine designers at the fore side of the turbine vanes. Also, in order to measure the validity of the results, the data gained from this study and the projects of Vakil and Thole [7] and Stitzel and Thole [21] were compared.

2 Research methodology

In the present study, the combustor simulator applied was a 3D representation of a Prat and Whitney gas turbine engine. As seen in Figure 1, the combustor was a 3D container. The model width, length and height were 111.7, 156.9 and 99.1 cm, respectively. The container converged from x/L=0.51 and contraction angle was 15.8 degrees. Inlet and outlet cross-sectional areas of the combustor simulator were 1.11 and 0.62 m^2, respectively.

The test section contained two symmetric surfaces on the top and bottom of the combustor, but the fluid flowed only through the bottom passage. The lengths of the cooling panels were 39, 41, 37 and 43 cm, respectively. In addition, the first two panels were flat and had constant sectional area. However, the last two panels were inclined at the contraction angle. The panels were 1.27 cm thick, and because of low thermal conductivity (k=0.037 W/m K), adiabatic surface temperature measurements were possible. Two different dilution rows were considered within the second and third cooling panels. The dilution flow was injected into the mainstream flow vertically, whereas the dilution hole in the third panel was angled at 15.8 degrees from the vertical axis. The first row of dilution jets included three holes and was placed at 0.67 m downstream of the combustor simulator inlet. These holes were 8.5 cm in diameter. The second row contained two dilution holes and was located at 0.23 m downstream of the first row of dilution holes' centre. The diameter of these holes was 1.4 times more than the first one at 12.1 cm. The centreline of the second row was staggered with respect to that of the first row. In the present research, the combustor simulator contained four arrangements of cooling holes. For the verification of findings, the first arrangement (baseline or case 1) was designed similar to the Vakil and Thole [7] combustor simulator. The length of these cooling holes was 2.5 cm and the holes were drilled at an angle of 30 degrees from the horizontal surface. The film-cooling holes

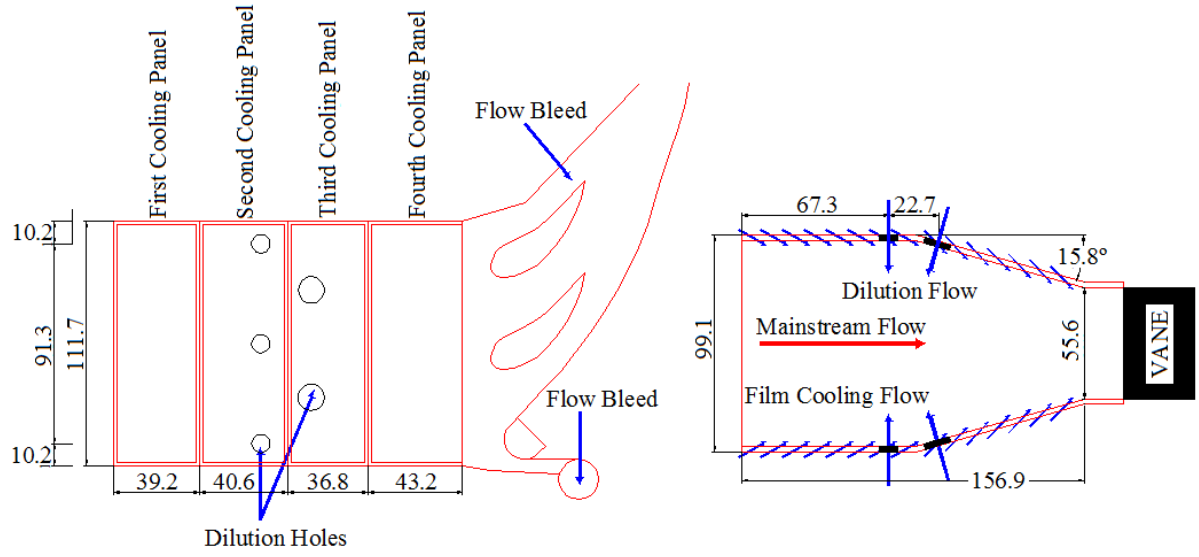

Figure 1: Schematic view of the combustor simulator

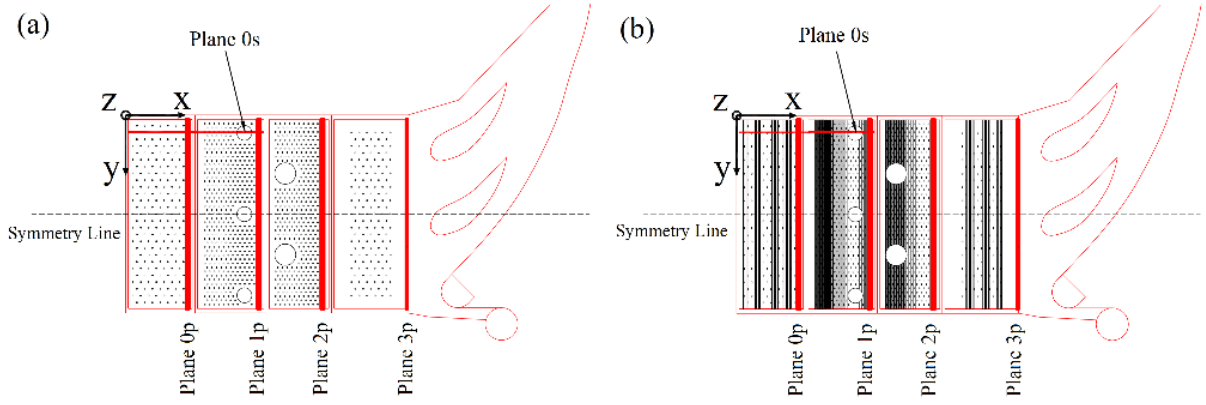

Figure 2: Location of the observation planes: (a) baseline, (b) case 2.

were 0.76 cm in diameter. Except the baseline case which was introduced, to investigate the effects of cooling holes trenching, row-trenched holes with alignment angle of 90 degrees with trench depth and width of, respectively, 0.75*D* and 1.0*D* were considered. Furthermore, coolant blowing ratio was BR=3.18. Therefore, the Cartesian coordinate system (*x*, *y* and *z*) was selected. The temperatures of coolant and dilution jets and mainstream flow were 295.5 and 332 K, respectively. Figure 2 shows the observation planes which are used to measure the film-cooling effectiveness distribution for baseline case and three different configurations of row-trenched cooling holes.

The observation planes of 0p, 1p, 2p and 3p and 0s were placed in pitchwise and streamwise directions, respectively. Plane 0p was located at x = 35.1 cm. The distribution of film-cooling momentum was computed along this panel. Plane 1p was located at the trailing edge of the first row of dilution jet. Plane 1p was developed from z = 0 cm to z = 10 cm and covered the whole width of the combustor simulator. It was applied to identify the effects of film cooling and dilution jets interaction, the horseshoe, half-wake and counter-rotating vortexes effects. Plane 2p was placed at the trailing edge of the second row of dilution jets. It was placed at x/L = 0.69 and was developed along the vertical axis. Plane 3p shown in Figure 3 was applied to determine the behaviour of outlet flow and varying combustor temperatures. At last, plane 0s was placed at the centre of the first row of dilution jet at y = 9.3 and extended from x = 39.2 cm to x = 78.45 cm. The importance of this plane was to identify the streamwise behaviour of the dilution jets in the first row. About 8×10^6 tetrahedral meshes were selected. The meshes were denser around the

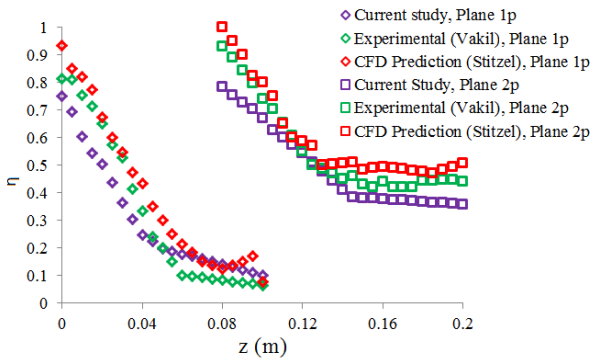

Figure 3: The film-cooling effectiveness comparison of planes 1p and 2p along $y/W = 0.4$.

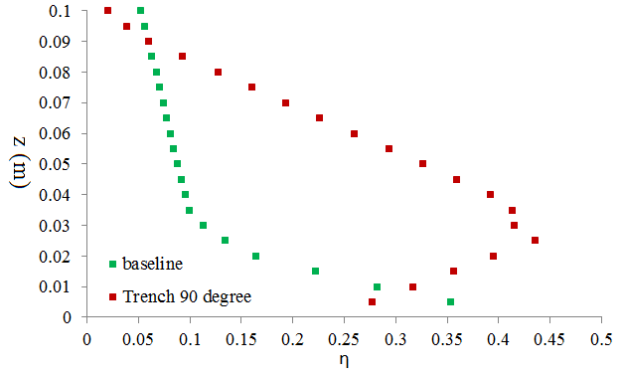

Figure 4: Film-cooling effectiveness at the intersection point of planes 1p and 0s.

cooling and dilution holes as well as wall surfaces. According to the considered blowing ratio at the inlet of control volume, the boundary condition of inlet mass flow was considered at the inlet. To limit the interaction region between fluid and combustor wall, slip-less boundary condition and wall boundary condition were considered. In addition, two different boundary conditions of uniform flow and pressure outlet were selected at the inlet and outlet of combustor, respectively. Totally, according to the symmetries of the Pratt and Whitney gas turbine engine combustor, the symmetry boundary condition was used. Gambit package was selected to mesh the combustor simulator and the model was analysed by FLUENT 6.2.26 software. The numerical method considered a transient, incompressible turbulent flow by means of the k–ϵ turbulent model of the Navier–Stokes equations expressed as follows:

Continuity equation:

$$\frac{\partial}{\partial t}(\rho u_i) + \frac{\partial}{\partial x_j} = \rho\left(u_i u_j\right) = -\frac{\partial P}{\partial x_i} + \frac{\partial \tau_{ij}}{\partial x_i} + \rho g_i + \vec{F}_1 \quad (1)$$

Momentum equation:

$$\frac{\partial}{\partial t} + \frac{\partial \rho}{\partial x}\frac{dx}{dt} + \frac{\partial \rho}{\partial y}\frac{dy}{dt} + \frac{\partial \rho}{\partial z}\frac{dz}{dt} = -\rho(\nabla . V) \quad (2)$$

Energy equation:

$$\frac{\partial}{\partial t}(\rho E) + \frac{\partial}{\partial x_i}(u_i(\rho E + P)) = \frac{\partial x}{\partial x_i}\left[K_{eff}\frac{\partial T}{\partial x_i} - \sum_j h_j J_j + u_j(\tau_{ij})_{erf}\right] + S_h \quad (3)$$

and k–ϵ equation:

$$\frac{\partial}{\partial t}(\rho k) + \frac{\partial}{\partial x_i}(\rho k u_i) = \frac{\partial}{\partial x_j}\left[\left(\mu + \frac{\mu_t}{\sigma_k}\right)\frac{\partial k}{\partial x_j}\right] + P_k - \rho\varepsilon \quad (4)$$

$$\frac{\partial}{\partial t}(\rho\varepsilon) + \frac{\partial}{\partial x_i}(\rho\varepsilon u_i) = \frac{\partial}{\partial x_j}\left[\left(\mu + \frac{\mu_t}{\sigma_\varepsilon}\right)\frac{\partial \varepsilon}{\partial x_j}\right] + C_{1\varepsilon}\frac{\varepsilon}{k}P_k - C^{\star}_{2\varepsilon}\rho\frac{\varepsilon^2}{k} \quad (5)$$

To investigate the convergence limit, the control volume mass residue was estimated and the maximum value has been used. For this research, the criterion of convergence chosen was 10^{-4}. The following equation is to determine the effectiveness of film cooling:

$$\frac{T - T_\infty}{T_c - T_\infty} \quad (6)$$

Here, T is the local temperature, and $T_\infty$and T_c are the temperatures of the mainstream and coolant, respectively.

3 Findings and discussion

The findings of the current research were compared with the experimental results of Vakil and Thole [7] and numerical findings gathered by Stitzel and Thole [21]. The effectiveness of film cooling was compared in plane 1p and 2p at $y/W = 0.4$. The deviations between the results of current research and benchmarks were computed by the following equation:

$$\%Diff = \frac{\frac{\sum_{i=1}^{n} x_i - x_{i,benchmark}}{x_{i,benchmark}}}{n} \times 100 \quad (7)$$

The deviation was equal to, respectively, 9.76% and 8.34% compared to Vakil and Thole measurements [7] and Stitzel and Thole [21] estimation for plane 1p and 13.36% and 11.96% in comparison with Ref. [7] and Ref. [21] for plane 2p (Figure 3).

Much of the film-cooling effectiveness data in this study were collected on the assumption that symmetry could be applied within the combustor simulator. Figure 4 shows a vertical film-cooling effectiveness distribution

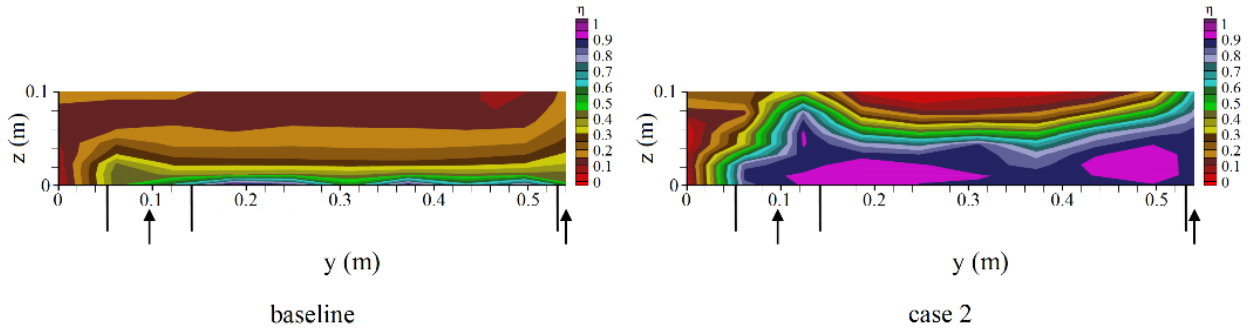

Figure 5: Film-cooling effectiveness for plane 1p.

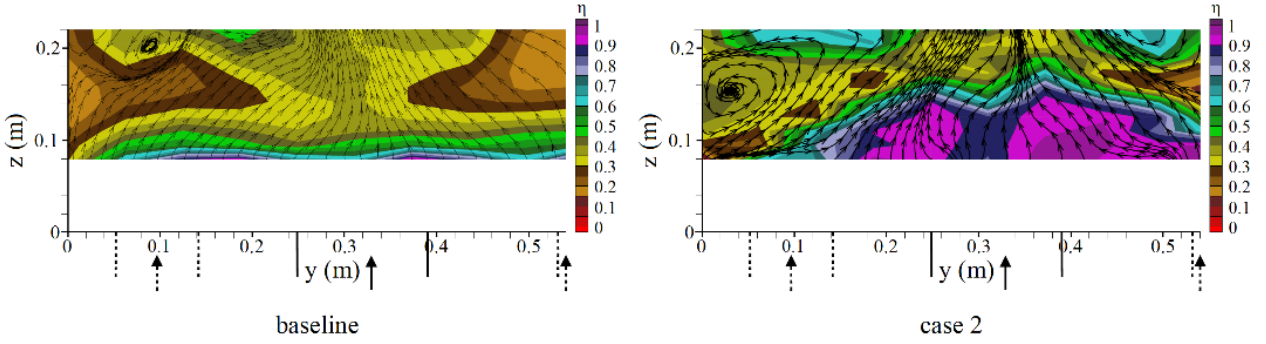

Figure 6: Vectors of *v* and *w* overlaying temperature contours within plane 2p.

taken at the intersection of panels 1p and 0s which extended over approximately 10% of the total inlet height at high blowing ratio of 3.18. The trailing edge footprints of both dilution jets can be seen in the figure.

According to Figure 4, as the film-cooling effectiveness reached $\eta = 0.353$ adjacent to the combustor end wall surface, the performance of the baseline case was understandably more efficient than the other one. As the vertical direction distance from the end wall surface grew larger, the cooling performance continuously reduced for both the baseline and the trenched holes with alignment angle of 90 degrees.

Figure 5 shows the findings related to film-cooling effectiveness of plane 1p at high blowing ratios, BR=3.18. Note that when film cooling significantly increased, the dilution jet injection remained the same. Figure 5 shows slightly higher levels near the wall for the trenched case relative to the baseline. However, no major improvements in cooling were observed along the liner wall. It was just downstream of the dilution jet and near the corners that the thermal field contours indicated that film cooling was being entrained by the upward motion of the dilution jet. Moreover, the temperature was slightly higher ($0 < \eta < 0.05$) for the trenched holes with alignment angle of 90 degrees at the position of 18 cm < y < 28 cm and 38 cm < y < 50 cm.

Figure 6 shows the contours of film-cooling effectiveness in plane 2p located one dilution hole diameter (1D2) downstream of the trailing edge of a dilution two hole. The injection of coolant into the mainstream is the basic difference between the obtained contours. Right at the trailing edge of the second row of dilution jets (10 cm < y < 50 cm) and at higher blowing ratios, the trenched holes created a protective layer ($0.9 < \eta < 1.0$) on the critical surfaces, which was more efficient than that of the baseline. A warmer area ($0.15 < \eta < 0.20$) expanded at the right (0 cm < y < 4 cm) and left (48 cm < y < 52 cm) sides of the thermal field contour. This figure shows the *v* and *w* velocity vectors superimposed on the top of the thermal field contours in plane 2p. It is visible for all arrangements that the coolant sweeps towards the second row of dilution jet and accelerates near the combustor wall. However, vectors such as dominant vortical structures hardly show any sign that might help with further mixing out of the non-uniform temperature field.

Figure 7 shows the effects of hole geometries on a streamwise film-cooling effectiveness distribution at BR=3.18. The results show that the trenched holes with alignment angle of 90 degrees performed the most effec-

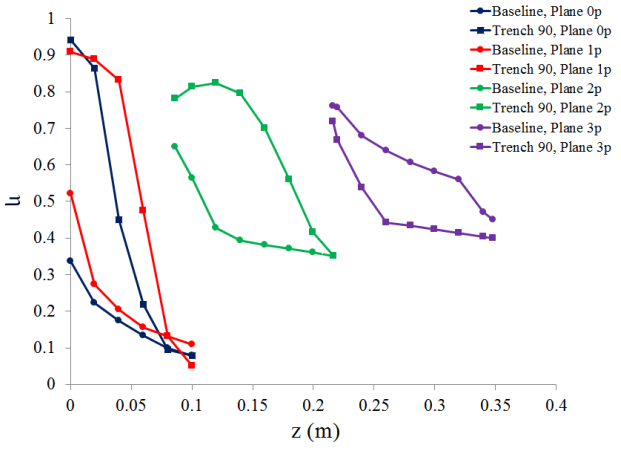

Figure 7: Effect of trenching cooling holes on film-cooling effectiveness distributions.

tively, especially in observation planes of 0p and 2p. This was 1.4 times as much the film-cooling effectiveness of the baseline case. At this blowing ratio, the film-cooling effectiveness of this kind of row-trenched cooling holes has fluctuations at 0 cm < z < 2 cm. The film exiting the trenches created a new boundary and enhanced heat transfer coefficients immediately downstream of the trench. In plane 3p, at BR=3.18 and because of the increase in the local interaction between mainstream and jets, both baseline and the trenched holes with alignment angle of 90 degrees produced almost similar effectiveness, that is, η = 0.76 and η = 0.718, respectively.

4 Conclusions

The commercial CFD code Fluent with RNG k–ϵ turbulence model was employed to analyse the effects of baseline case and row-trenched cooling holes with different alignment angles under blowing ratio of 3.18. Compared to baseline method, in the trenched case, the coolant stayed closer to the end wall surface and did not allow main entrainment. It also provided significant lateral spreading and stronger coverage. Film cooling was also explored at high blowing ratios and the observation plane of 0p and 2p, using trenched holes with alignment angle of 90 degrees. For plane 1p, at the trailing edge of the second cooling panel, the row-trenched holes with alignment angle of 90 degrees increased film-cooling effectiveness by 75%, which is much higher than the baseline case. Comparisons between the data computationally predicted and those collected by Vakil and Thole [15] and Stitzel and Thole [21] indicate the existence of similarities and differences. The predicted thermal field data indicated an under-predicted measurement for the current study as opposed to the experimental findings. An optimized design cooling holes will help to maximize the effectiveness of cooling along the combustor end wall surface and prevent premature wear in this area.

References

[1] **Salimi, S., Fazeli, A. and Kianpour, E.**: Film Cooling Effectiveness Using Cylindrical and Compound Cooling Holes at the End Wall of Combustor Simulator, *Journal of Advanced Research in Fluid Mechanics and Thermal Sciences,* 1(1), **2014**, 38-43.

[2] **Abdullah, K. and Funazaki K.I.**: *Effects of Blowing Ratio on Multiple Angle Film Cooling Holes,* AEROTECH IV Conference, Kuala Lumpur, Malaysia, **2012**.

[3] **Sarkar, S. and Bose, T.K.**: Numerical simulation of a 2-D jet-crossflow interaction related to film cooling applications: Effects of blowing rate, injection angle and free-stream turbulence, *Sadhana,* 20(6), **1995**, 915-935.

[4] **Nasir, H., Ekkad, S.V. and Acharya, S.**: Effect of compound angle injection on flat surface film cooling with large streamwise injection angle, *Exp Therm Fluid Sci,* 25(1-2), **2001**, 23-29.

[5] **Shine, S.R., Sunil Kumar, S. and Suresh, B.N.**: Internal wall-jet film cooling with compound angle cylindrical holes, *Energ Convers Manage,* 68, 2013, 54–62.

[6] **Hale, C.A., Plesniak, M.W. and Ramadhyani, S.**: Film Cooling Effectiveness for Short Film Cooling Holes Fed by a Narrow Plenum, *J Turbomach,* 122(3), **2000**, 553-557.

[7] **Vakil, S.S. and Thole, K.A.**: Flow and Thermal Field Measurements in a Combustor Simulator Relevant to a Gas Turbine Aero engine, *J Eng Gas Turb Power,* 127(2), **2005**, 257 -267.

[8] **Kianpour, E., Sidik, N. A. C. and Wahid, M. A.**: Cylindrical and Row Trenched Cooling Holes with Alignment Angle of 90º at Different Blowing Ratios, *CFD Letters,* 5(4), **2013**, 165-173.

[9] **Kianpour, E. and Sidik, N. A. C.**: Computational investigation of film cooling from cylindrical and row trenched cooling holes near the combustor endwall, *Case Studies in Thermal Engineering*, 4, **2014**, 76-84.

[10] **Somawardhana, R.P. and Bogard, D.G.**: Effects of obstructions and surface roughness on film cooling effectiveness with and without a transverse trench, *J Turbomach,* 131(1), **2009**, 011010-1-011010-8.

[11] **Harrison, K.L., Dorrington, J.R., Dees, J.E., Bogard, D.G. and Bunker, R.S.**: Turbine Airfoil Net Heat Flux Reduction With Cylindrical Holes Embedded in a Transverse Trench, *J Turbomach,* 131(1), **2009**, 011012-1-011012-8.

[12] **Shuping, C.**: Film cooling enhancement with surface restructure, PhD Thesis. University of Pittsburgh, **2008**.

[13] **Yiping, L. and Ekkad, S.V.**: *Predictions of film cooling from cylindrical holes embedded in trenches,* 9th AIAA/ASME Joint Thermophysics and Heat Transfer Conference, California, **2006**.

[14] **Ai, W., Laycock, R.G., Rappleye, D.S., Fletcher, T.H. and Bons, J.P.**: Effect of particle size and trench configuration on deposition from fine coal flyash near film cooling holes, *Energ Fuel,* 25(3), **2011**, 1066–1076.

[15] **Zhang, X. Z. and Hassan, I.**: Numerical investigation of heat transfer on film cooling with shaped holes, *Int J Heat Fluid Fl,* 16(8), **2006**, 848-869.

[16] **Gao, Z., Narzary, D. and Han, J.C.**: Turbine Blade Platform Film Cooling With Typical Stator-Rotor Purge Flow and Discrete-Hole Film Cooling, *J Turbomach,* 131(4), **2009**, 041004-1-041004-11.

[17] **Colban, W., Thole, K.A. and Haendler, M.**: A comparison of cylindrical and fan-shaped film-cooling holes on a vane end wall at low and high freestream turbulence levels, *J Turbomach,* 130(3), **2008**, 031007-1-031007-9.

[18] **Saumweber, C., Schulz, A. and Wittig, S.**: Free- Stream Turbulence Effects on Film Cooling With Shaped Holes, *J Turbomach,* 125(1), **2003**, 65-73.

[19] **Saumweber, C. and Schulz, A.**: Free-stream effects on the cooling performance of cylindrical and fan-shaped cooling holes, *J Turbomach*, 134(6), **2012**, 061007-1-061007-12.

[20] **Barigozzi, G., Franchini, G., Perdichizzi, A. and Ravelli, S.**: Film cooling of a contoured end wall nozzle vane through fan-shaped holes, *Int J Heat Fluid Fl,* 31(4), **2010**, 576-585.

[21] **Stitzel, S. and Thole, K.A.**: Flow field computations of combustor-turbine interactions relevant to a gas turbine engine, *J Turbomach,* 126(1), **2004**, 122-129.